SENSITIVITY ANALYSIS OF THE PETROPHYSICAL PROPERTIES VARIATIONS ON THE SEISMIC RESPONSE OF A CO2 STORAGE SITE

Juan E. Santos

Instituto del Gas y del Petróleo, Facultad de Ingeniería UBA and Department of Mathematics, Purdue University and Universidad Nacional de La Plata

Work in collaboration with: G. B. Savioli (UBA), L. A. Macias (UBA), J. M. Carcione and D. Gei (OGS)

INTRODUCTION I

➢ Injection of CO2 in deep saline aquifers is a procedure used for reducing the amount of greenhouse gases in the atmosphere.

➢ This work studies CO2 injection into the Utsira formation at the Sleipner gas field. The Utsira sandstone is a highly permeable porous medium with several mudstone layers which act as barriers to the vertical upward flow of CO2.

➢ First, pressure and CO2 saturation maps are generated using a multiphase fluid flow simulator. Then, time lapse seismic is used to determine the spatio-temporal distribution of CO2 applying a viscoelastic wave propagation simulator.

INTRODUCTION II

➢ The petrophysical model of the Utsira formation assumes fractal porosity and clay content, taking into account the variation of properties with pore pressure and saturation.

➢ Since CO_2 injection changes the porosity and permeability flow parameters, a sensitivity analysis is performed to determine the time step at which such parameters need to be updated.

➢ The wave propagation simulator takes into account mesoscopic loss effects due to the presence of CO_2 within the Utsira sand.

➢ The frequency dependent Lamè parameters at the macroscale are determined from the pressure and saturation maps computed by the flow simulator.

METHODOLOGY

➢ Use a Black-Oil multiphase fluid flow numerical simulator to model CO_2 injection into the Utsira formation at the Sleipner field.

➢ Include variations in flow parameters due to changes in pressure and saturation

➢ Use a wave propagation simulator including mesoscopic loss effects to monitor the spatio-temporal distribution of CO_2 in the formation.

The basic concepts and ideas used in this presentation can be found in the book

Numerical Simulation in Applied Geophysics

by Juan Santos and Patricia Gauzellino, Birkhauser, 2016

SEG

INTERNATIONAL EXPOSITION AND 87TH
ANNUAL MEETING
HOUSTON·TEXAS
24-29 SEPTEMBER 2017

BLACK OIL MODEL OF BRINE-CO2 FLOW I

Mass conservation equation (g = CO2 , w = brine)

$$-\nabla \cdot \left(\frac{1}{B_g}\bar{v}_g + \frac{R_s}{B_w}\bar{v}_w\right) + q_g = \frac{\partial\left[\phi\left(\frac{S_g}{B_g} + \frac{R_s S_w}{B_w}\right)\right]}{\partial t}$$

$$-\nabla \cdot \left(\frac{1}{B_w}\bar{v}_w\right) + q_w = \frac{\partial\left[\phi\frac{S_w}{B_w}\right]}{\partial t}$$

ϕ: porosity S_i: phase i saturation p_i: phase i pressure q_i: flow rate per unit volume

i = g, w

R_s: gas solubility in water B_g: gas formation volume factor

B_w: water formation volume factor

Darcy's Empirical Law (g = CO2 , w = brine)

$$\bar{v}_g = -\bar{\bar{K}}\frac{k_{rg}}{\eta_g}\left(\nabla p_g - \rho_g g \nabla z\right)$$

$$\bar{v}_w = -\bar{\bar{K}}\frac{k_{rw}}{\eta_w}\left(\nabla p_w - \rho_w g \nabla z\right)$$

$$S_w + S_g = 1 \qquad p_g - p_w = P_C(S_g)$$

$\bar{v}_i =$ Darcy velocity $\bar{\bar{K}}$: absolute permeability tensor η_i: phase i viscosity

$k_{ri}(S_i)$: phase i relative permeability $P_C(S_g)$: gas-water capillary pressure

BLACK OIL MODEL OF BRINE-CO2 FLOW III

➢ The numerical solution is obtained employing the public domain software BOAST.

➢ BOAST solves the flow differential equations using IMPES (IMplicit Pressure Explicit Saturation), a finite difference technique.

➢ The basic idea of IMPES is to solve:
   ✓ A pressure equation: obtained combining the flow equations for both phases.
   ✓ A saturation equation: flow equation for the brine phase.

IMPES TECHNIQUE

➢ The IMPES system is linearized evaluating the pressure and saturation dependent coefficients at the previous time step.

➢ The pressure equation is solved implicitly, applying a Block Successive Over Relaxation method (BSOR).

➢ The saturation equation is solved explicitly, therefore stability restrictions are considered to select the flow time step.

MESOSCOPIC LOSS AND WAVE PROPAGATION SIMULATIONS I

➢ A dominant P-wave attenuation mechanism in reservoir rocks at seismic frequencies is due to wave-induced fluid flow (WIFF, mesoscopic loss).

➢ Fast P and S-waves travelling through mesoscopic-scale heterogeneities (larger than the pore size but smaller than the wavelength), induce fluid flow and slow (diffusion) Biot waves by mode conversion.

➢ The wave propagation simulator used at the macroscale allows to represent the mesoscopic loss mechanism

MESOSCOPIC LOSS AND WAVE PROPAGATION SIMULATIONS II

➢ In zones where CO2 is present, the complex and frequency dependent P-wave modulus at the macroscale

$$E(\omega) = \lambda(\omega) + 2\mu(\omega)$$

is determined using White's theory for patchy saturation (White et al., Physics of Solid Earth, 1975)

$\lambda(\omega)$, $\mu(\omega)$: Lamè coefficients, ω: angular frequency.

➢ Shear wave attenuation is taken into account using another relaxation mechanism, related to the P-wave White mechanism.

MESOSCOPIC LOSS AND WAVE PROPAGATION SIMULATIONS III

➢ In zones where only brine is the saturating fluid, the complex bulk and shear moduli as function of frequency were determined using a Zener model.

These complex moduli define an equivalent viscoelastic model at the macroscale that takes into account dispersion and attenuation effects occurring at the mesoscale

SEISMIC MODELING. A VISCOELASTIC MODEL FOR WAVE PROPAGATION

Equation of motion in a 2D isotropic viscoelastic domain :

$$\omega^2 \rho \, \mathbf{u} + \nabla \cdot \sigma(\mathbf{u}) = f(x, \omega), \quad \Omega$$

$$-\sigma(\mathbf{u})\nu = i\,\omega\,\mathbf{D}\,\mathbf{u}, \quad \partial\Omega$$

$f(x, \omega)$ = external source   D: positive definite matrix

The solution of the viscoelastic wave equation was computed at a selected number of frequencies in the range of interest using an iterative Finite Element (FE) domain decomposition procedure.

The formation is a uniform shaly sand with clay content C = 6% and initial fractal porosity.

The pressure dependence of properties of the flow parameters is defined by the relation between porosity ϕ (t) and pore pressure $p(t) = S_w \, p_w(t) + S_g \, p_g(t)$ (Carcione et al., J. Appl. Physics, 2003),

$$\frac{1 - \phi_c}{K_s}(p(t) - p_H) = \phi_0 - \phi(t) + \phi_c \ln\left(\frac{\phi(t)}{\phi_0}\right)$$

ϕ_c: critical porosity K_s: bulk modulus of solid grains

p_H = hydrostatic pressure ϕ_0: initial porosity

THE PARAMETERS OF THE FLUID FLOW AND SEISMIC MODELS II

➢ The relationship among horizontal permeability k_x, ϕ and C is (Carcione et al., 2003),

$$\frac{1}{k_x(t)} = \frac{45(1 - \phi(t))^2}{\phi(t)^3} \left(\frac{(1 - C)^2}{R_q^2} + \frac{C^2}{R_c^2} \right)$$

R_q: radius of sand grains R_c: radius of clay grains

➢ As permeability is anisotropic, the following relationship between horizontal k_x and vertical permeability k_z is assumed:

$$\frac{k_x(t)}{k_z(t)} = \frac{1 - (1 - 0.3a)\sin(\pi S_w)}{a(1 - 0.5\sin(\pi S_w))}$$

a: permeability anisotropy parameter

The Krief equation (Krief et al., The Log Analyst, 1990) is used to determine the bulk and shear moduli of the dry matrix, K_m, μ_m :

$$K_m(t) = K_s(1 - \phi(t))^{A/(1-\phi(t))} \qquad \mu_m(t) = \mu_s(1 - \phi(t))^{A/(1-\phi(t))}$$

Using the moduli K_s, K_m, μ_m, the porosity ϕ and permeabilities k_x, k_z, as well as the fluids bulk moduli and viscosities, in zones where CO2 is present the complex and frequency dependent plane wave modulus $E(\omega)$ was determined using White's theory for patchy saturation (White et al., 1975)

NUMERICAL EXAMPLES I

➢ Consider a 2D section of the Utsira formation with 1.2 km in the x-direction and 0.4 km in the z-direction (top at 0.77 km and bottom at 1.17 km b.s.l.)

➢ Within the formation, there are several low permeability mudstone layers, but with openings giving a path for the upward migration of CO_2.

➢ CO_2 is injected at a constant flow rate of one million tons per year. The injection point is located at the bottom of the formation: x = 0.6 km, z=1.082 km (Arts et al., First Break, 2008).

➢ The flow simulator uses a uniform mesh of 300 cells in the x-direction and 400 cells in the z-direction.

NUMERICAL EXAMPLES II – The flow functions
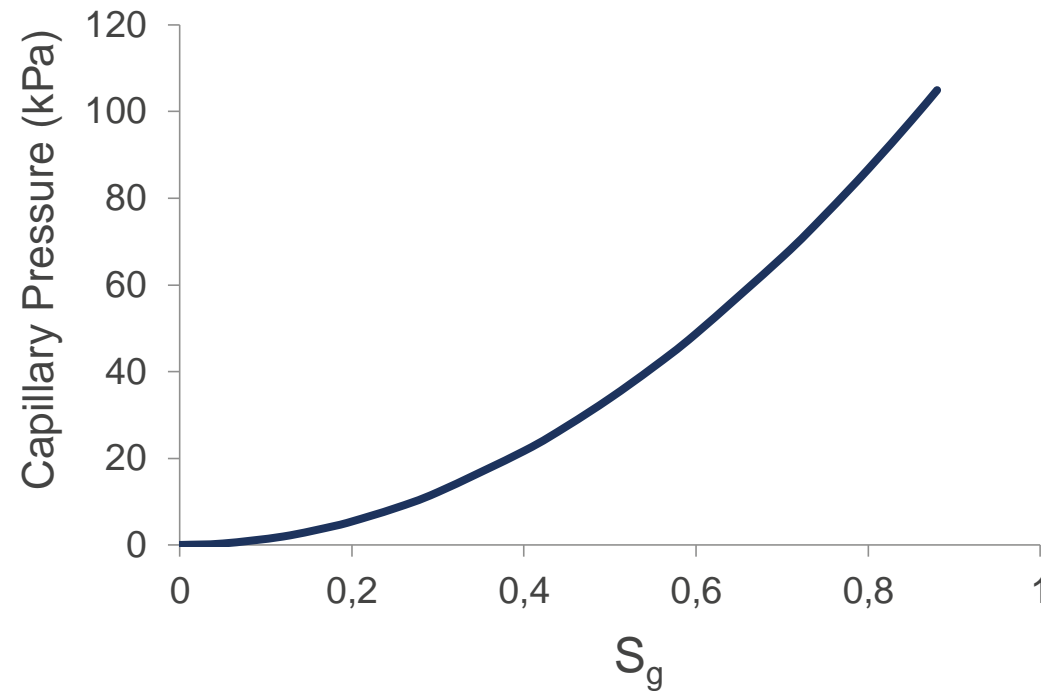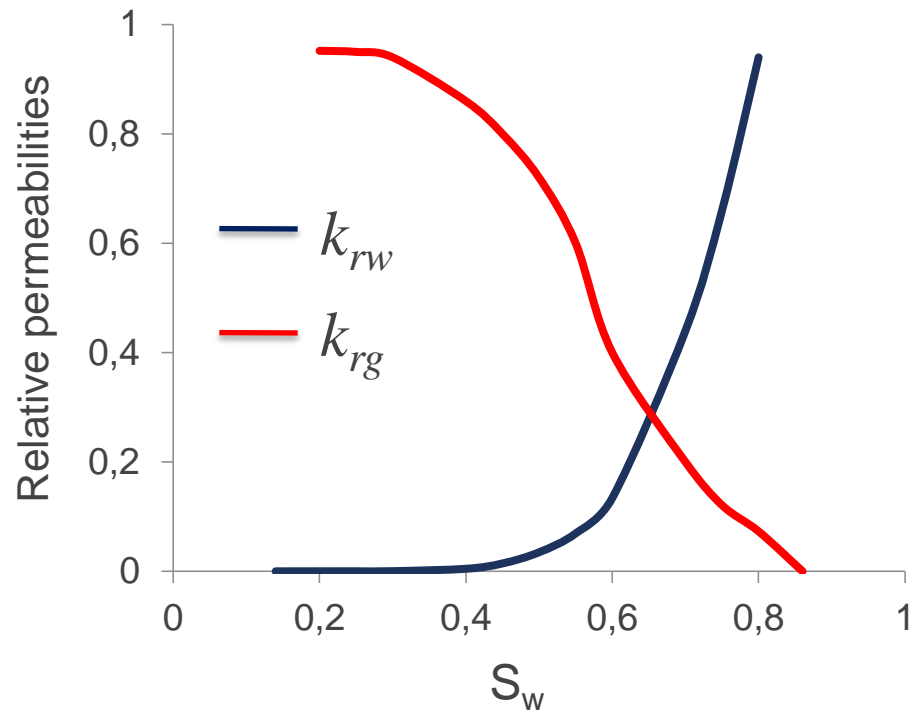
NUMERICAL EXAMPLES III

➢ During the CO2 injection simulation, significant changes in (k, ϕ) occur at times much larger than the flow time step Δt_f . Thus we need two levels of temporal discretizations:

1) A flow time step Δt_f = 0.08 day satisfying the CFL stability condition, to solve the flow equations.

2) A formation time step Δt_g at which the flow parameters (k, ϕ) depending on pressure and saturation are updated.

Thus numerical experiments are performed to determine the largest Δt_g at which the results of the flow simulations (pressure and saturation) remain essentially unchanged.

Sensitivity analysis for different Δt_g and 1 year of injection
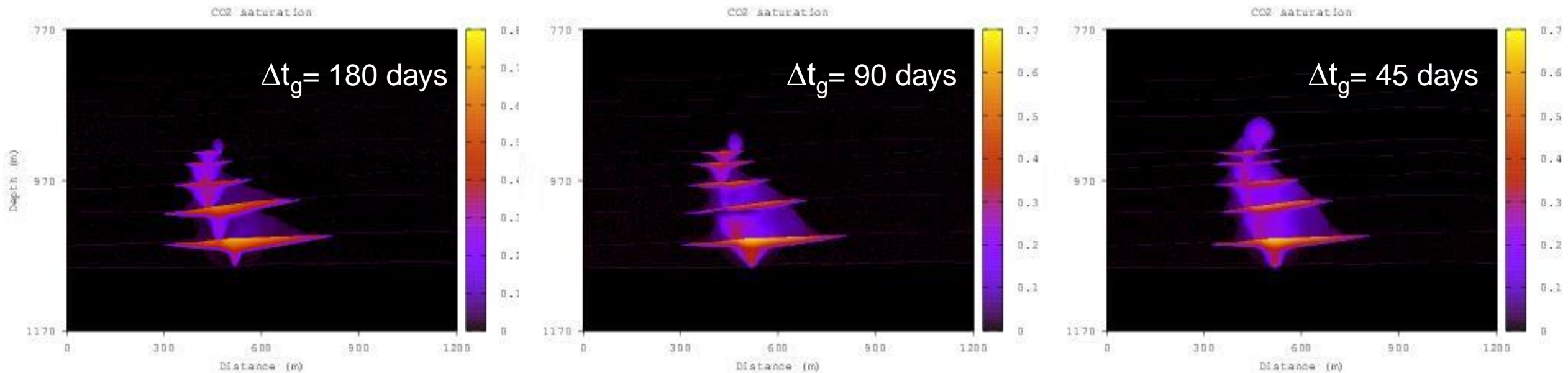
Because k_z is saturation dependent, the CO2 plume is seen to move upwards faster when the petrophysical properties are updated more frequently, i.e., as Δt_g is reduced

Saturation maps after two years of CO2 injection
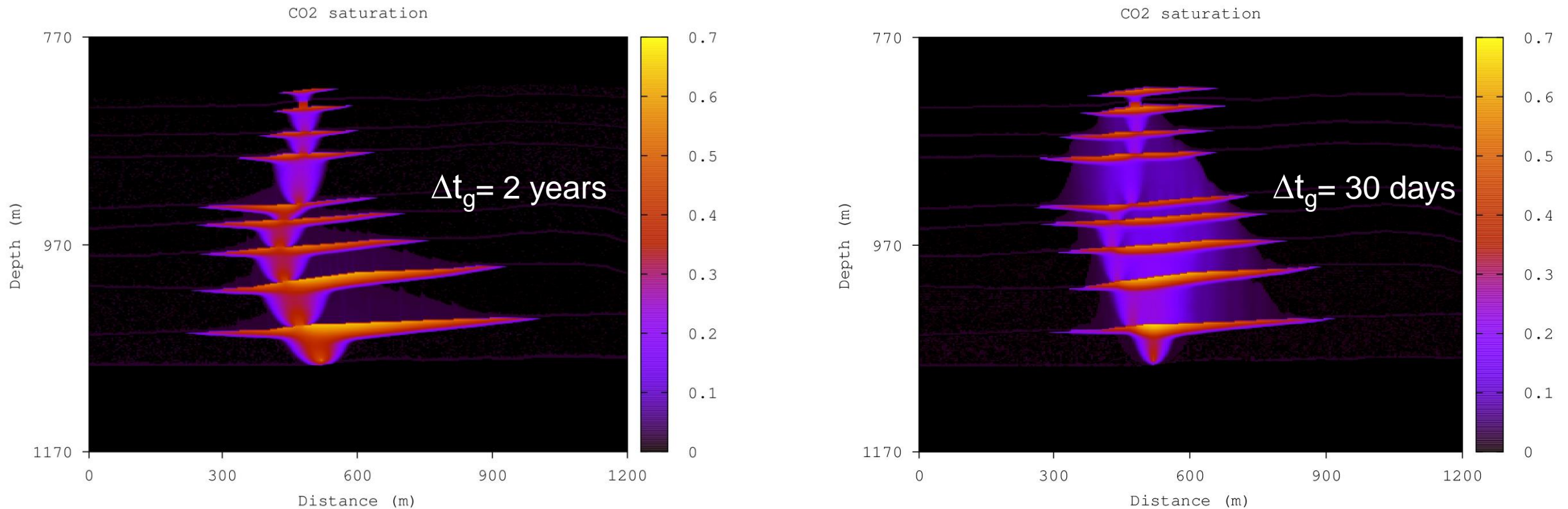
The left figure, obtained without updating flow parameters, shows very well defined chimneys and accumulations below the mudstone layers. The right figure, computed updating every 30 days, displays a less defined chimney, thinner accumulations and more extended CO2 zones between mudstone layers.

Saturation maps after two years of CO2 injection
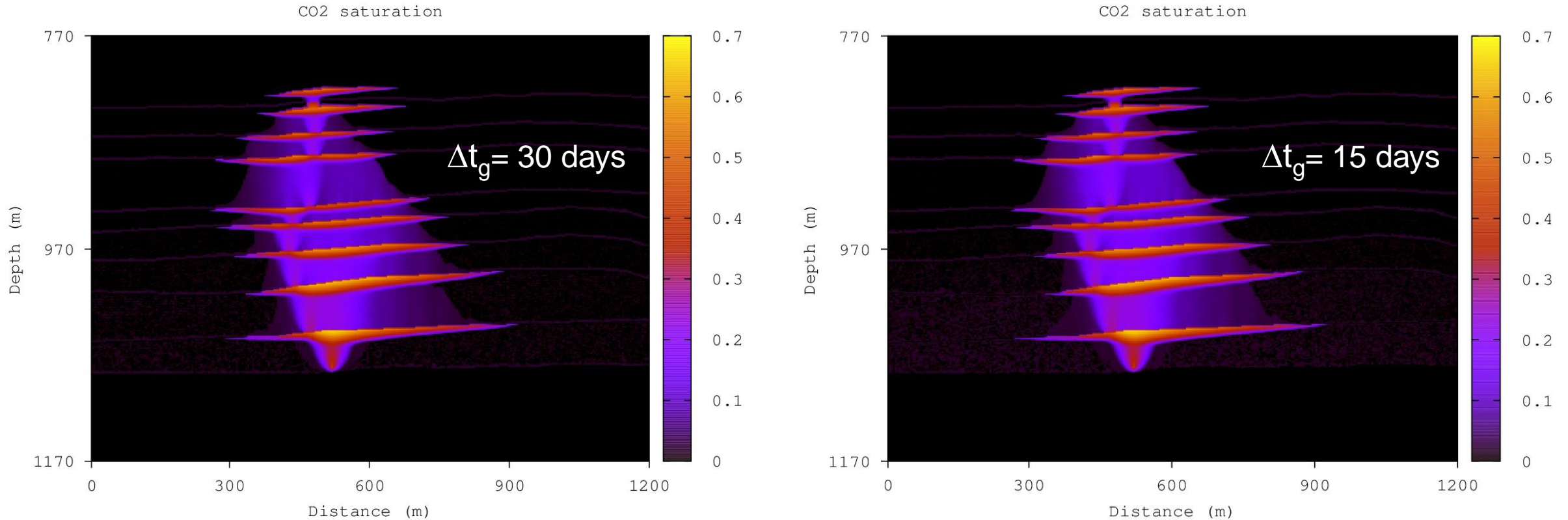
These two very similar figures show that it is enough to use a formation time step $\Delta\mathbf{t}_g$ of 30 days to update the parameters (k, ϕ) in the flow simulator.

The quadratic relative error between the two maps is about 0.22%

Time Lapse Seismic applied for monitoring CO2 injection I

➢ We apply the wave propagation simulator to analyze the effect of updating the petrophysical and seismic properties in the synthetic seismograms.

➢ The simulator includes mesoscopic loss effects associated with the presence of CO2 as injection proceeds, as described above.

CO2 saturation and synthetic seismogram after 1 year of injection without updating parameters
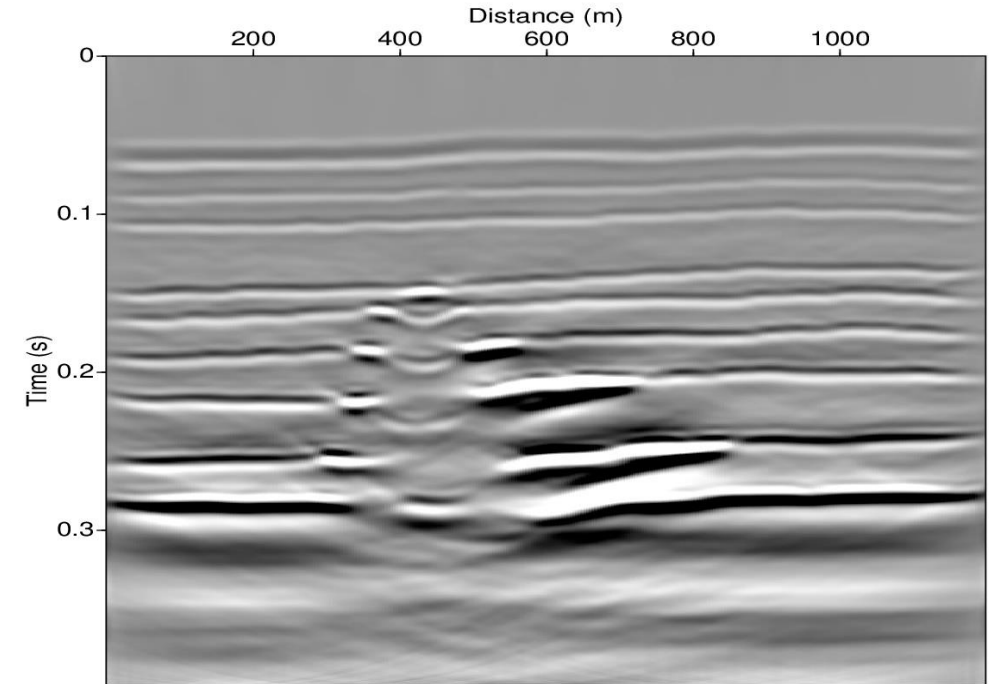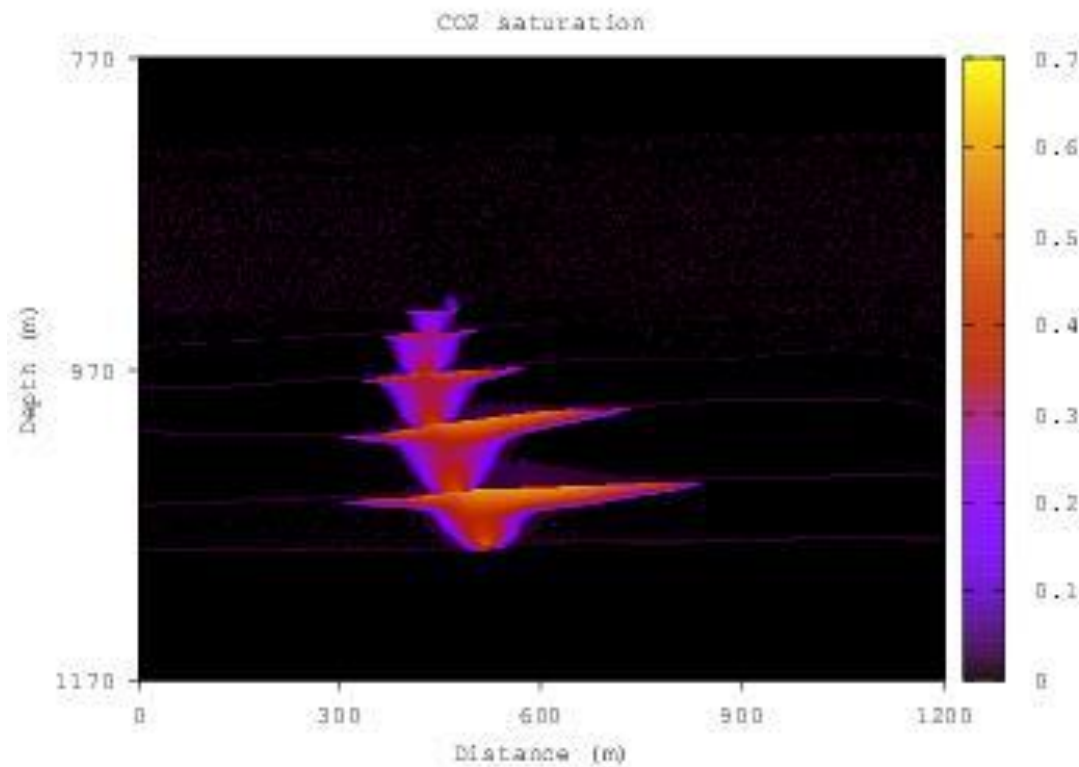
The CO2 plume induces the pushdown effect

CO2 saturation and synthetic seismogram after 1 year of injection updating parameters every 30 days
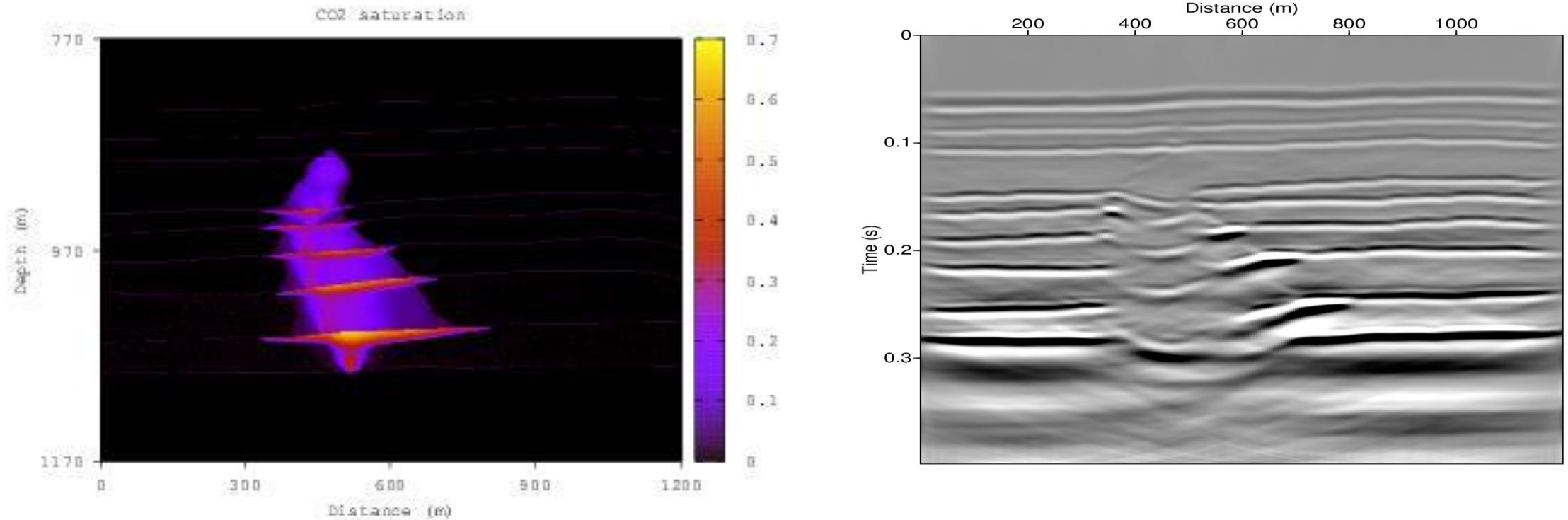
The pushdown effect is better observed when the simulation parameters are updated every 30 days

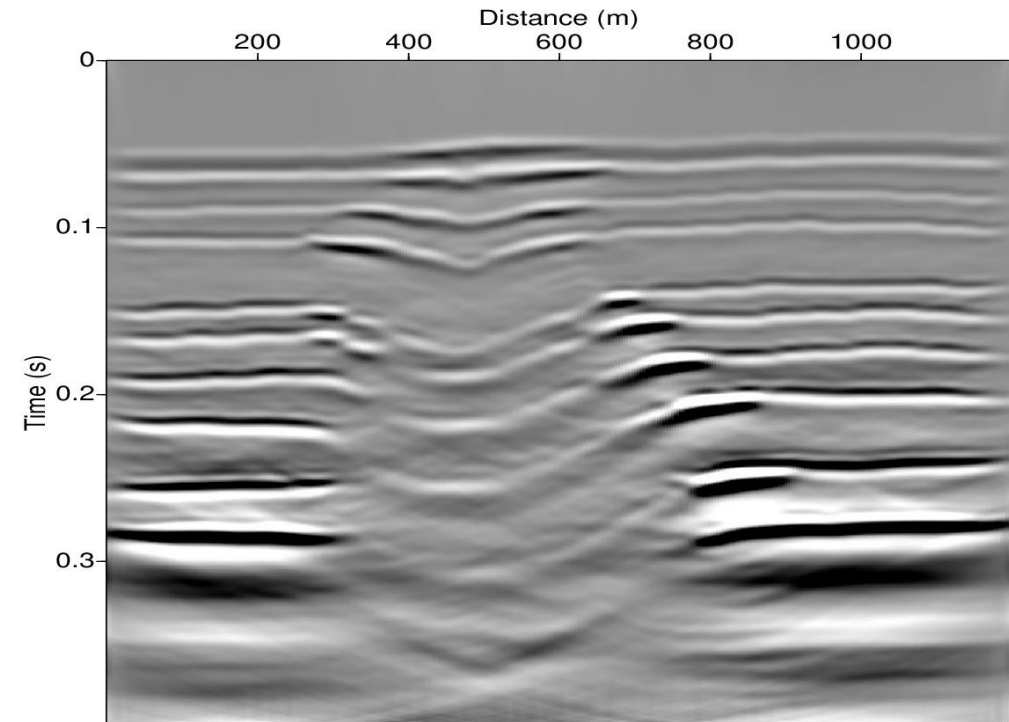# Synthetic seismogram after 1 year of injection without and with updating parameters
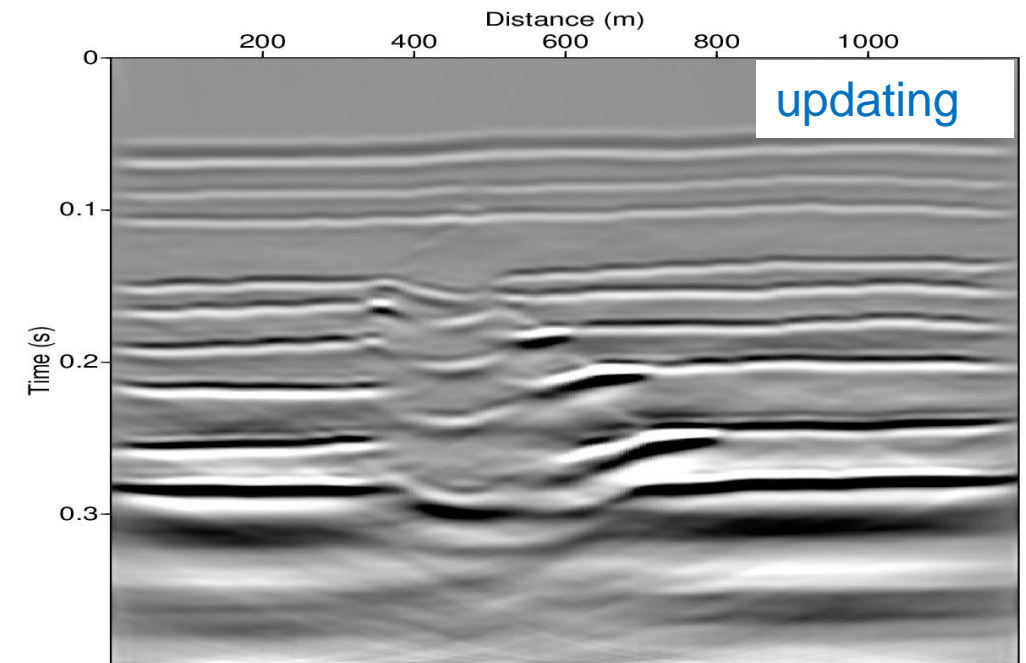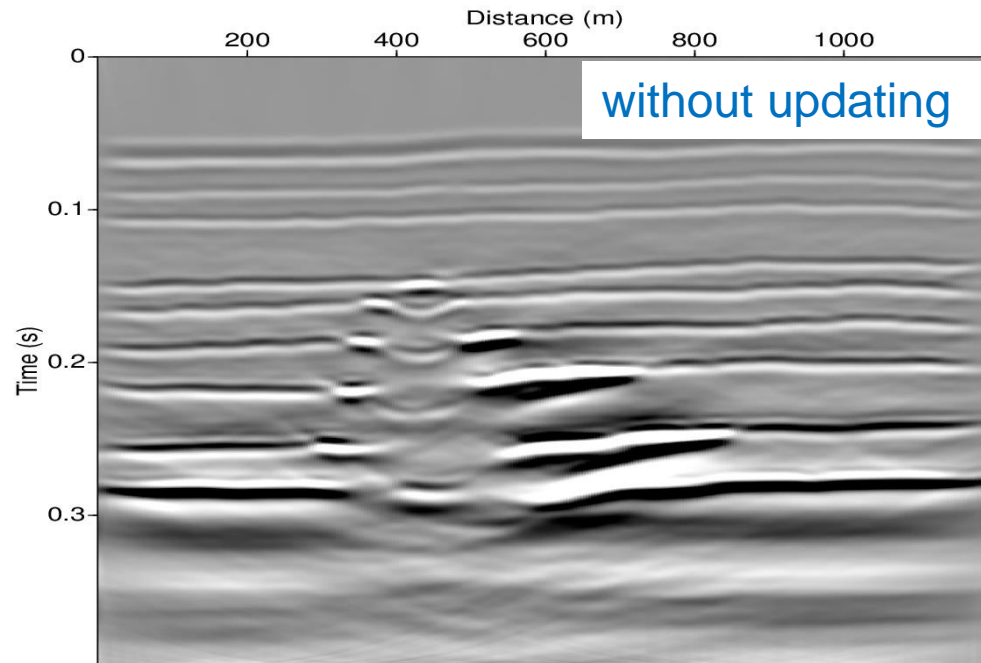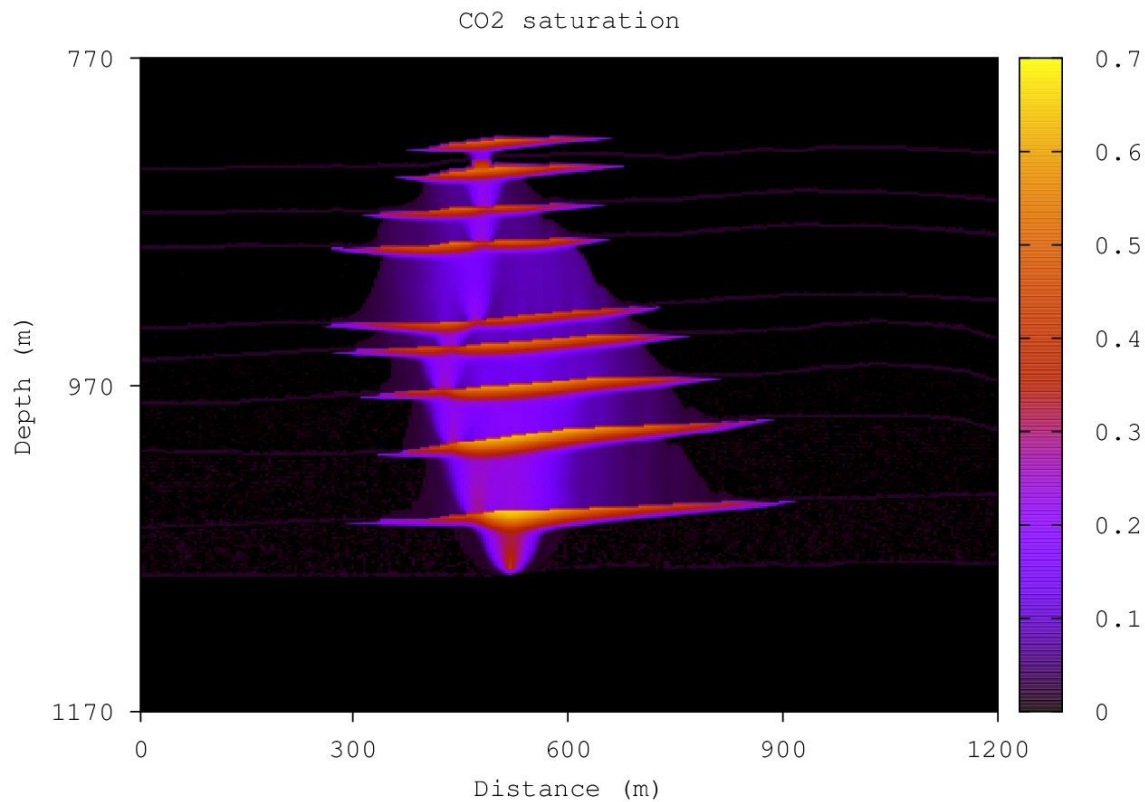

When the simulation parameters are updated (right figure) the CO2 plume induces the pushdown effect in a wider region in the horizontal direction, and moves faster in the vertical direction as compared with the left figure, obtained without updating parameters
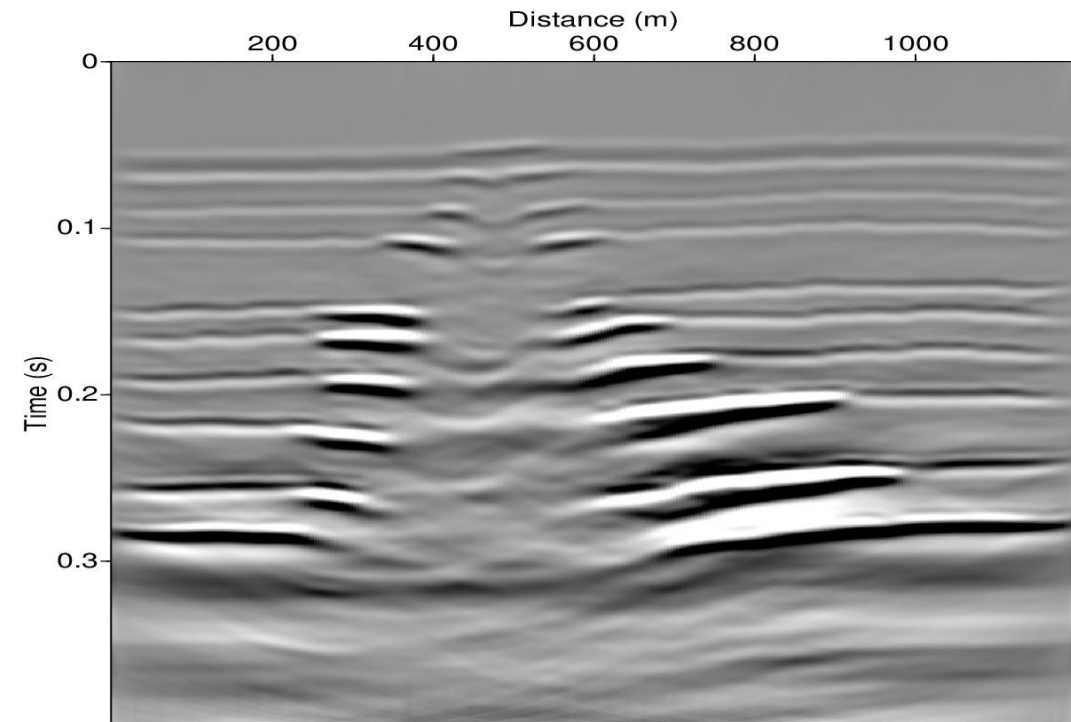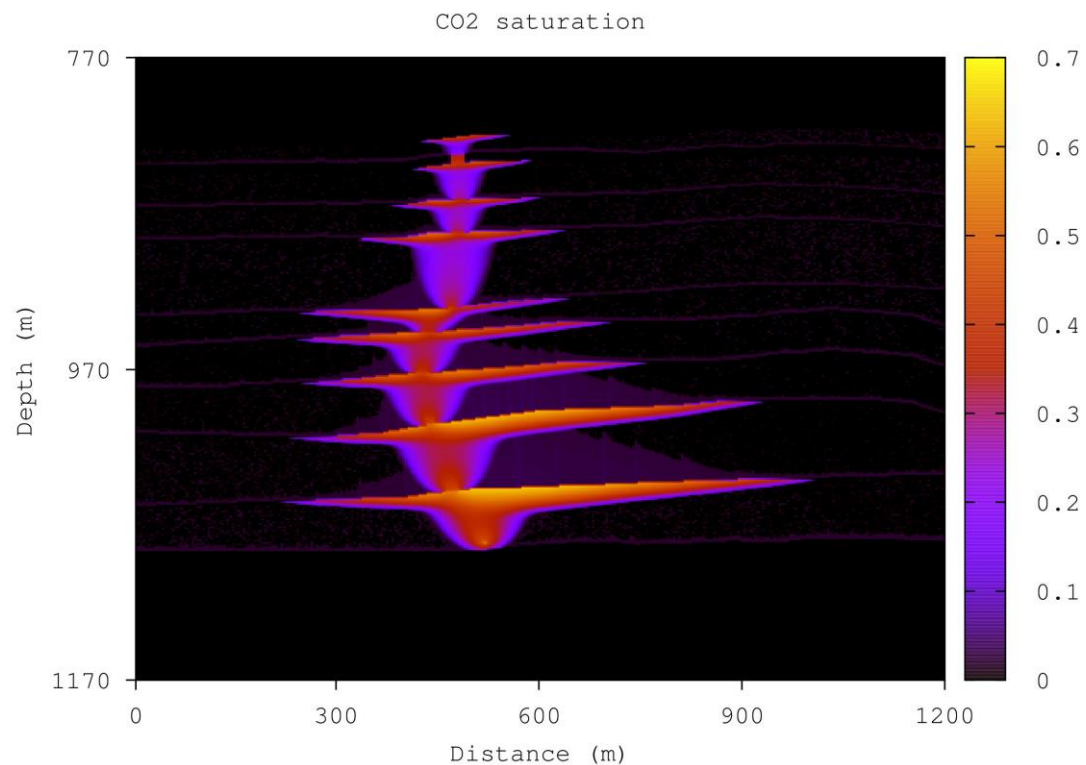
CO2 saturation and synthetic seismogram after 2 years of injection without updating parameters
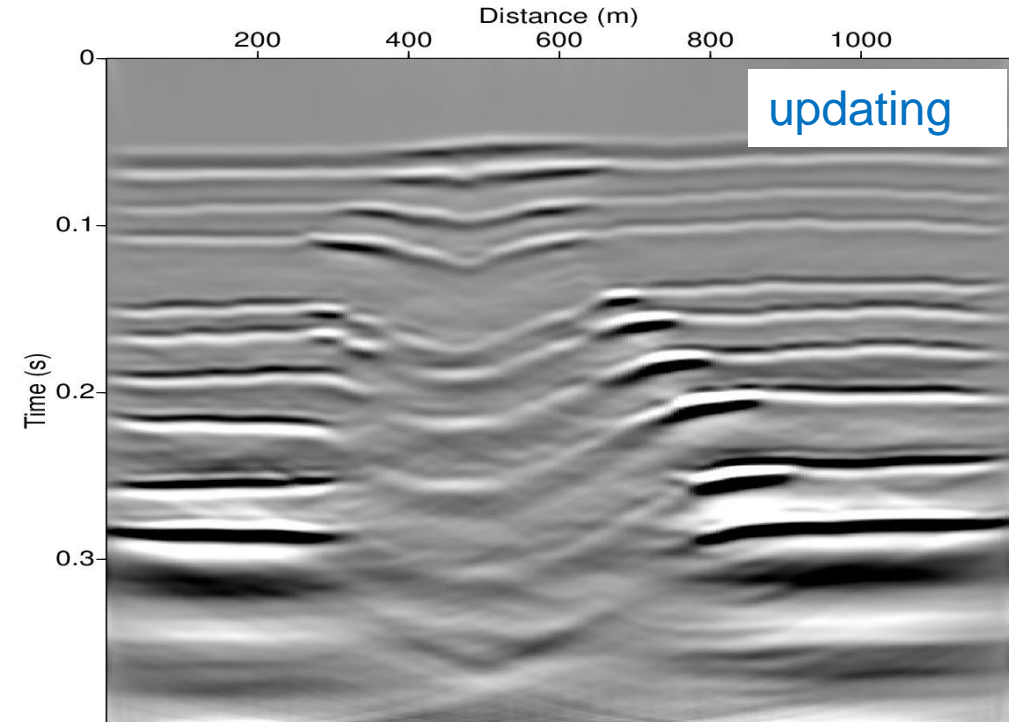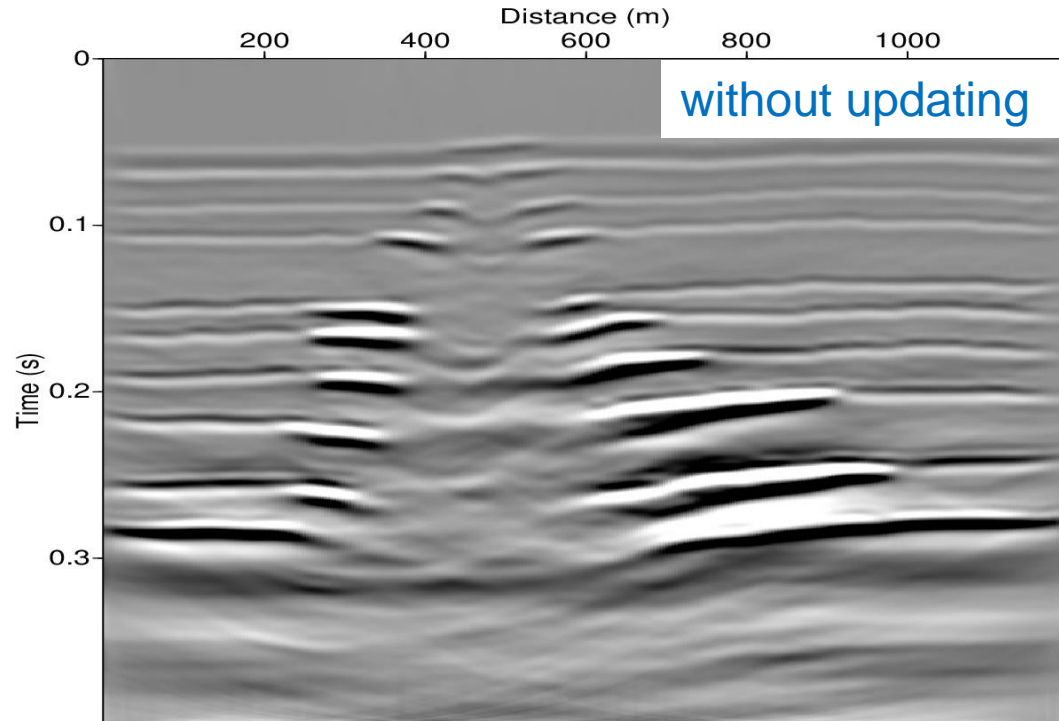
CO2 saturation and synthetic seismogram after 2 years of injection updating parameters every 30 days

Synthetic seismogram after 2 years of injection without and with updating parameters every 30 days

Again, the CO2 plume moves faster in the vertical direction and induces the pushdown effect in a wider region in the horizontal direction when the petrophysical and seismic properties are updated

CONCLUSIONS I

➢ We presented a methodology to determine the flow and formation time steps to apply time lapse seismics for monitoring CO_2 injection in saline aquifers.

➢ The methodology, when applied to the Utsira formation, yielded a suitable formation time step of 30 days.

➢ Using this formation time step to update the simulation parameters allowed to obtain accurate seismic images of the spatial distribution of CO_2 after injection.

CONCLUSIONS

- ➢ Furthermore, a precise definition of the zone where the pushdown effect occurs is obtained.

- ➢ The delay observed in the pushdown region, of about 50 ms, is in good agreement with that measured in real data (Chadwick et al., Proc. 6th Petroleum Geology Conference, 2005).

THANKS FOR YOUR ATTENTION !!!!